

ESTIMATION OF EFFECTIVE TEMPERATURE OF AN ARTIFICIAL QUANTUM TWO-LEVEL SYSTEM

Pavol Neilinger¹, Matúš Rehák¹ and Miroslav Grajcar^{1,2}

¹*Dept. of Exp. Physics, FMFI, Comenius University, 84248 Bratislava, Slovakia*

²*Institute of Physics, Slovak Academy of Sciences, Bratislava, Slovakia*

E-mail: neilinger@fmph.uniba.sk

Received 12 May 2015; accepted 20 May 2015

1. Introduction

Quantum electrodynamics (QED) studies the interaction of photons and matter. In atomic cavity QED an isolated atom interacts with the quantized electromagnetic modes inside a high quality optical cavity. An alternative to the atomic optical cavity QED [1] is the circuit QED, where artificial quantum two-level systems are coupled to high quality microwave superconducting resonators[2,3,4]. Circuit QED enables to study and repeat fundamental experiments of quantum physics and QED on a solid state chip. As these artificial quantum two-level systems are promising candidate for quantum computers they are often labeled as quantum bits or qubits.

A superconducting flux qubit is a solid-state electrical circuits consisting of a micrometer sized superconducting loop interrupted by several Josephson junctions [5,6,7]. The external tuning parameter is the magnetic flux Φ in the loop and the qubit is represented by a generally asymmetrical double-well potential. Two classical states $|0\rangle$ and $|1\rangle$ are defined by the direction of the circulating persistent current I_p in the loop (or equally, magnetic flux pointing up and magnetic flux pointing down). The two states are coupled by quantum-mechanical tunneling through the barrier separating the wells leading to superposition of the two classical states [8]. The qubit energy splitting between the ground $|g\rangle$ and excited state $|e\rangle$, which is an equivalent to atomic-transition energy in optics, is then

$$\hbar\omega_q = \sqrt{\Delta^2 + \varepsilon^2}, \quad (1)$$

where Δ is the minimum energy level splitting for externally applied magnetic flux $\Phi = \Phi_0/2$ (the degeneracy point). The energy bias of the qubit ε , which is similar to the Zeeman splitting, depends on the external magnetic flux as $\varepsilon=2I_p(\Phi - \Phi_0/2)$.

The interaction of the quantized electromagnetic field of the resonator and the qubit is described by the Jaynes-Cumming Hamiltonian

$$H = \frac{\hbar\omega_q}{2}\sigma_z + \hbar\omega_r\left(a^\dagger a + \frac{1}{2}\right) + \hbar g_\varepsilon(a^\dagger\sigma^- + a\sigma^+), \quad (2)$$

where g_ε is the normalized qubit-resonator coupling, ω_r is the resonator frequency, σ_z is the Pauli spin matrices in the qubit eigenbasis, a (a^\dagger) is the annihilation (creation) operator of the resonator photon field and σ_- (σ_+) is the lowering (raising) operator of the qubit. For simplicity, here we neglected the damping terms.

Two different regimes are of special interest, the resonant and the dispersive regime [2]. In the resonant regime the qubit energy-level splitting is in resonance with the resonator frequency and a direct exchange of excitations without energy loss between these two systems is possible. In the dispersive regime, for large detuning between the qubit and the resonator ($g_\varepsilon/\delta \ll 1$, where $\delta = \omega_q - \omega_r$), direct excitation sharing is not possible. However, as a consequence of the qubit-resonator interaction the energy levels of the qubit and the resonator are mutually affected. The energy-level splitting of the qubit depends on the cavity

state, and vice versa. The diagonalization of the Hamiltonian E.g.1 in the second order in g_e/δ leads to [9]:

$$H = \hbar \left(\omega_r + \frac{g^2}{\delta} \sigma_z \right) a^\dagger a - \frac{\hbar}{2} \left(\omega_q + \frac{g^2}{\delta} \right) \sigma_z. \quad (3)$$

This relation directly shows a dispersive shift in the resonator energy (first term). If the qubit is in the ground state, the resonator frequency is lowered by $-g_e^2/\delta$, whereas for excited qubit the frequency of the resonator is increased by $+g_e^2/\delta$. This state dependency of the dispersive shift enables to use the resonator as a read-out of the qubit state.

In this paper we present a time averaged continuous wave measurement of a qubit-resonator system spectrum near the qubit degeneracy point. Two dispersive shifts in the spectrum of the resonator are observed and identified as corresponding to the ground and excited state of the qubit, as a consequence of finite qubit temperature. The different transmission amplitudes of the resonator at these shifts are utilized to estimate the temperature of the qubit.

2. Design and fabrication

A pair of superconducting flux qubits were placed in the middle of a niobium $\lambda/2$ coplanar waveguide resonator's centre line (see Fig. 1a)). The resonator was fabricated by conventional sputtering and dry etching of a 150-nm-thick niobium film. The patterning uses electron-beam lithography and a CF_4 ion-etching process. The resonator was design to work in over-coupled regime, to ensure sufficiently high transmission [4]. The fundamental resonance frequency of the resonator was designed to 2.5 GHz. The aluminum qubits were fabricated by shadow evaporation technique. Each qubit consisting of a superconducting loop interrupted by 6 Josephson junctions [11], was strongly coupled to the resonator by a large shared Josephson junction. Moreover, the qubits were mutually coupled by a Josephson junction (Fig. 1a)). The dimensions of the qubit's Josephson junctions are $0.2 \times 0.3 \mu\text{m}^2$, $0.2 \times 0.2 \mu\text{m}^2$, and $0.2 \times 0.3 \mu\text{m}^2$, the critical current density is about $200 \text{A}/\text{cm}^2$, and the area of the qubit-loop is $5 \times 4.5 \mu\text{m}^2$.

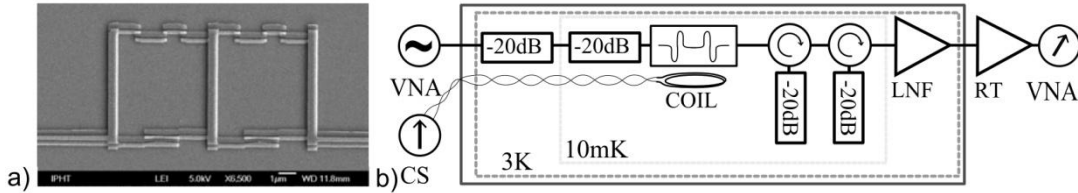


Fig.1: a) SEM image of the aluminium qubits in the resonator. b) Scheme of the rf-experimental set-up in the refrigerator.

3. Experimental set-up

The experiment was carried out in a cryogen-free dilution refrigerator with base temperature of 10 mK. The sample was glued and wire-bonded to a printed circuit board with $50 \mu\text{m}$ aluminum wires and enclosed in a copper box. The scheme of the rf-experimental set-up is in Fig. 1b). On the input line, where a weak probing signal at frequency $\omega_s \sim 2\pi \times 2.481$ GHz was applied (VNA N5242A), a set of thermally anchored attenuators were placed at 3K stage and mixing chamber stage (10mK) of the refrigerator. On the output line, a cryogenic circulator was installed between the sample and low noise cryogenic amplifier (LNF) placed on 3 K plate in order to isolate the sample from the thermal noise (Fig. 2a) and amplify the signal. The output signal was further amplified by a low-noise room temperature amplifier (RT) (+36dB) and the signal was detected by vector network analyzer (VNA N5242A,

homodyne detection). The qubit was biased by dc magnetic field provided by a single superconducting coil fixed to the sample holder.

4. Results

The transmission of the resonator was measured by a vector network analyzer for a weak probing ($p_p = -141$ dBm, corresponding to a mean photon number in the resonator $n \approx 5$). The fundamental frequency and the quality factor of the resonator were determined to be $\omega_r \sim 2\pi \times 2.481$ GHz and $Q \sim 18\,000$, respectively (corresponding to bandwidth of $BW \sim 2\pi \times 140$ KHz). The dependence of the resonator's resonance frequency on the applied external magnetic field is showed in Fig. 2a). Here two dispersive shifts (Eq. 3) in the resonance frequency can be identified, corresponding to the two qubits. For the two-qubit sample, due to the inhomogeneity of the applied magnetic field, the effective magnetic flux for each of the qubits is different, which allows to treat the qubits for certain applied magnetic fields as single ones. The shift in the resonant frequency is negative as is expected for qubits in ground state. The dispersive shift is dependent on the qubit resonator detuning and is the largest at the qubit degeneracy point (Eq. 3). The magnetic field set by the current in the bias loop is calibrated to Φ_0 by measuring several periods of the qubits. However, due to the insufficient isolation and filtering on the input/output lines and coil's bias current, one expects the temperature of the qubit to be higher than the ambient temperature determined by the temperature of mixing chamber (10 mK). The finite temperature of the qubit would give rise to finite probability of the qubit to be in the excited state, and thus the resonator should have finite transmission at positively shifted frequency, if the qubit relaxation rate is much lower than the photon escape rate out of the resonator.

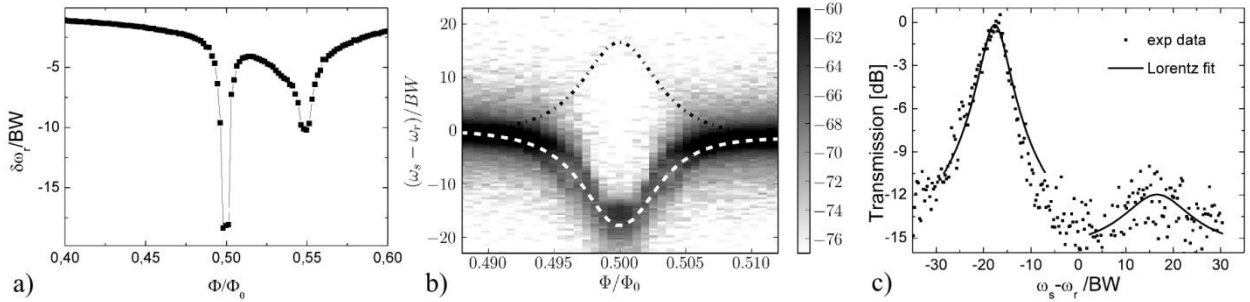


Fig.2: a) The dependence of the resonator's resonance frequency shift $\delta\omega_r$, on the normalized applied external magnetic field Φ/Φ_0 . b) The transmission spectrum of the resonator in dependence of the magnetic field. The dashed/dotted line corresponds to the negative/positive dispersive shift of the resonator frequency for the qubit in the ground/excited state according to Eq. 3. for the estimated qubit parameters. c) Transmission spectra of the resonator along cross-section at the qubit degeneracy point $\Phi/\Phi_0=0.5$. The transmission amplitudes were estimated from fit to Lorentzian curve

Indeed, a close look at the plot of the resonator transmission spectrum on dependence of the magnetic field reveals branching of the resonance frequency with two branches corresponding to the ground and excited state of the qubit. A cross section in Fig. 2c) shows two resonance peaks at frequencies with different transmissions. Here we define the transmission amplitude ratio of the two transmission peaks as the ratio of the resonator transmission amplitude A_+/A_- in linear scale at $\omega_r \pm g_c^2/\delta$. The density matrix at thermal equilibrium is characterized by the Boltzmann distribution

$$\rho(T_{eff}) = \begin{pmatrix} \rho_{gg} & 0 \\ 0 & \rho_{ee} \end{pmatrix} = \frac{1}{Z} \begin{pmatrix} \exp(-\hbar\omega_q/2k_bT_{eff}) & 0 \\ 0 & \exp(\hbar\omega_q/2k_bT_{eff}) \end{pmatrix}, \quad (4)$$

where $Z = \exp(-\omega_q/2k_bT_{eff}) + \exp(\omega_q/2k_bT_{eff})$, is the partition function, k_b is the Boltzmann constant and T_{eff} is the effective temperature of the qubit [12]. Assuming the transmission of the resonator in the two branches to be directly proportional to the thermally distributed populations of the qubit, the transmission amplitude ratio is related to the effective temperature of the qubit as $A_+/A_- = \exp(-\omega_q/k_bT_{eff})$. Thus, the transmission amplitude ratio enables to estimate the effective temperature of the qubit for known qubit parameters.

The qubit parameters $\Delta=2\pi\times 5.2$ GHz, $I_p = 140$ nA and $g = 80$ MHz were determined from the fit of the transmission spectra measured at third harmonics of the resonator (at resonant qubit-resonator interaction, for details see [10]) and are in good agreement with the dispersive measurement, as is showed in Fig. 2b). The transmission amplitude ratio $A_+/A_- = 1/15$ was obtained from Lorentzian curve fit of the resonance peaks at the qubit degeneracy point $\Phi/\Phi_0 = 0.5$. The estimated effective temperature of the qubit for these parameters is $T_{eff} = 93$ mK.

5. Conclusion

In this paper we have presented a simple estimation of the effective temperature of a quantum two level system (qubit) strongly coupled to a superconducting coplanar waveguide resonator. The experiment was carried out in a He³-He⁴ dilution refrigerator at temperature $T_{MC} = 10$ mK. The effective temperature of the qubit $T_{eff} \approx 93$ mK was estimated from time averaged measurement of the qubit-resonator transmission spectra. This estimate is in very good agreement with the noise temperature of the resonator $T_{res} \approx 105$ mK independently obtained from noise power spectral density measurement of the resonator (not presented here) and is slightly higher than the estimation from the known set of thermally anchored attenuators ($T_{Att} \approx 60$ mK [13]), which is expected according to imperfect cooling of the center conductor of the coaxial cables and filtering of the bias current of the coil. Moreover, the branching of the resonator resonant frequency in this experiment is a nice demonstration of the quantum nature of this system as this would not be possible for a classical system.

Acknowledgement

The research leading to these results has received funding from the European Community's Seventh Framework Programme (FP7/2007-2013) under Grant No. 270843(iQIT). This work was also supported by the Slovak Research and Development Agency under the contract APVV -0088-12, DO7RP-0032-11 and LPP-0159-09.

References:

- [1] H. Walther et al., Rep. Prog. Phys. 69 1325 (2006)
- [2] A. Blais et al., Phys. Rev. A **69**, 062320 (2004)
- [3] A. Wallraff et al., Nature **431**, 162 (2004)
- [4] M. Göppl et al., J. Appl. Phys. 104, 113904 (2008)
- [5] J. E. Mooij et al., Science, **285**, 1036 (1999)
- [6] J. R. Friedman et al., Nature **406**,43–46 (2000)
- [7] C. H. van der Wal et al., Science **290**,773–776 (2000)
- [8] J. Clarke et al., Nature **453**, 19 (2008)
- [9] A.N. Omelyanchouk et al., Low Temp. Phys. **36**, 893 (2010)
- [10] Nelinger et al., Phys. Rev. B **91**, 104516 (2015)
- [11] Rehak et al., Applied Physics Letters **104**, 162604 (2014)
- [12] M.Grajcar et al., Phys. Rev. Lett. **96**,047006 (2006)
- [13] P. Horowitz, W. Hill: The art of electronics, Cambridge University Press (1989)